IEEE Access
Multidisciplinary ⋮ Rapid Review ⋮ Open Access Journal

Received 2 August 2023, accepted 20 August 2023, date of publication 25 August 2023, date of current version 30 August 2023.

Digital Object Identifier 10.1109/ACCESS.2023.3308851

THEORY

The Output Regulation and the Kalman Filter as the Signal Generator

JESÚS ALBERTO MEDA-CAMPAÑA[1], (Member, IEEE), RAÚL EDUARDO TORRES-CRUZ[1], ALEXIS JESUS ROJAS-RUIZ[1], RICARDO TAPIA-HERRERA[2], (Member, IEEE), TONATIUH HERNÁNDEZ-CORTÉS[3], AND LUIS ALBERTO PÁRAMO-CARRANZA[4]

[1]SEPI-ESIME Zacatenco, Instituto Politécnico Nacional, Ciudad de México 07738, Mexico
[2]CONACYT-SEPI-ESIME Zacatenco, Instituto Politécnico Nacional, Ciudad de México 07738, Mexico
[3]Department of Mechatronics, Universidad Politécnica de Pachuca, Zempoala 43830, Mexico
[4]ESIME Zacatenco, Instituto Politécnico Nacional, Ciudad de México 07738, Mexico

Corresponding author: Jesús Alberto Meda-Campaña (jmedac@ipn.mx)

This work was supported in part by Consejo Nacional de Humanidades, Ciencias y Tecnologías (CONAHCYT), through the Scholarship Sistema Nacional de Investigadores (SNI); in part by Instituto Politécnico Nacional through Research Project under Grant 20230023; in part by the Scholarship Estímulo al Desempeño de los Investigadores (EDI); in part by the Scholarship Comisión de Operación y Fomento de Actividades Académicas (COFAA); and in part by the Scholarship Beca de Estímulo Institucional de Formación de Investigadores (BEIFI).

ABSTRACT In this work, the problem of following references and rejecting disturbances that are contaminated with noise and whose dynamics are too complex to have a mathematical model that describes the behavior of such signals is studied. In addition to exploiting the capabilities of the Kalman filter (KF) to clean the signals so that they can serve as external signals for the regulation theory, the construction of the generating system (exosystem) is proposed as a diagonal system by blocks, where each block is a Kalman filter that estimates each one of the corresponding reference/disturbance signals. The viability of the approach is verified by two examples, mimicking the problem of tracking a flying object moving freely in the 3D space by a quadrotor which is under the influence of the proposed controller when the displacements of the arbitrary flying object are measured by low-cost sensors.

INDEX TERMS Kalman filter, regulation theory, system identification, stochastic systems.

I. INTRODUCTION

The vast majority of signal measurement systems introduce random disturbances, which often causes such measurements to be filtered before they can be used. To deal with this kind of signals, the Kalman filter, which is an optimal state estimator for dynamic systems involving random disturbances, has been successfully applied in many areas of industrial and scientific fields, such as video and laser tracking systems, satellite navigation, ballistic missile trajectory estimation, radar, and fire control [1]. Clearly, having the possibility of measuring a signal does not imply that the mathematical model that describes the signal behavior is available. This situation affects the application of the Kalman filter because it requires the model of the system whose states are to be estimated/filtered. But, if the signal to be estimated/filtered can be assumed to have a behavior corresponding to a polynomial of degree n, then a linear system of dimension $n+1$ can be used as the mathematical model of such a signal [2], [3]. On the other hand, the problem of asymptotically taking the output of a given nonlinear plant toward a family of reference signals, while possibly, another family of disturbance signals is rejected, considering that both kinds of signals are generated by an external system (exosystem), still is interesting because it finds application in many fields of science and engineering [4], [5]. This control problem is named ''the nonlinear regulator problem'' and it is equivalent to finding the solution of a set of nonlinear partial differential equations, known as the Francis-Byrnes-Isidori equations (FBI equations). Furthermore, ''the linear regulator problem'' is equivalent to finding the solution of a set of some linear algebraic equations known as the Francis equations [6]. The main advantage of designing a nonlinear/linear regulator is that once such a controller is designed, it can track/reject

The associate editor coordinating the review of this manuscript and approving it for publication was Dong Shen.

all of the signals generated by the exosystem, despite the initial conditions of the external generator. At the same time, the main disadvantage is finding the exosystem capable of generating adequate reference/disturbance signals. Therefore, if the reference/disturbance signals are measurable, but there is no exosystem to describe them, then the "classical" regulation theory cannot be used. This disadvantage has been partially overcome in [7], [8], and [9]. In [7], the authors use an extended High-Gain Observer (HGO) to estimate the states of the plant, the external disturbances, and the feed-forward term necessary to track the reference. Then, in [8] and [9], the regulation theory is applied under the assumption that the reference/disturbance signals are nonmodeled but measurable for all $t \geq 0$, smooth, and bounded, which allows a High-Gain Observer to be used as the exosystem. Also in [8] and [9], the existence of the regulator was defined based on the solution of a modified set of Francis equations.

Although both of the mentioned works solved the best possible case, i.e., when the measures are noise-free, it is well-known the performance of the HGOs decays drastically when the reference/disturbance signals are tainted with noise [10].

Therefore, the problem studied in the present work is the tracking/rejecting of non-modeled reference/disturbance signals, which are contaminated with white noise. In that sense, the main contribution of this work is to extend the regulation theory to the area of nonmodeled reference/disturbance signals by the inclusion of a Kalman filter as an exosystem.

II. MATHEMATICAL TOOLS

A. KALMAN FILTER

Considering the nonlinear system

$$\dot{x}(t) = f(x(t), u(t)),$$
$$y(t) = h(x(t)),$$

where $x(t) \in \mathbb{R}^n$ is the vector state of the plant, $u(t) \in \mathbb{R}^p$ is the input vector of the plant, and $y(t) \in \mathbb{R}^m$ is the output vector of the plant, and the discrete-time linear system formed by the matrices $A_k = \frac{\partial f_d}{\partial x_k}$, $B_k = \frac{\partial f_d}{\partial u_k}$, $C_k = \frac{\partial h_d}{\partial x_k}$, with k as the discrete-time instant, $x_k \in \mathbb{R}^n$ as the state vector, $u_k \in \mathbb{R}^p$ as the input vector, $y_k \in \mathbb{R}^m$ as the output vector, and $f_d(\cdot,\cdot,\cdot)$ and $h_d(\cdot)$ as the discretizations of the continuous-time nonlinear funtions $f(\cdot,\cdot)$ and $h(\cdot)$, respectively. Then, the Kalman filter [1], [11], consists of a recursive algorithm through which an optimal estimator of states for a linear stochastic system is computed based on the least squares method [12]. Such an estimation process is divided into two sub-process: 1) Prediction and 2) Correction. Let the linear stochastic system be

$$x_{k+1} = A_k x_k + B_k u_k + \xi_k, \tag{1}$$
$$y_k = C_k x_k + \eta_k, \tag{2}$$

with $\xi_k \in \mathbb{R}^n$ as the dynamic noise with zero mean and variance $D_k \in \mathbb{R}^{n\times n}$, and $\eta_k \in \mathbb{R}^m$ as the measurement noise with zero mean and variance $M_k \in \mathbb{R}^{m\times m}$. Where, $A_k \in \mathbb{R}^{n\times n}$, $B_k \in \mathbb{R}^{n\times p}$, $C_k \in \mathbb{R}^{m\times n}$, $D_k \in \mathbb{R}^{n\times n}$and $M_k \in \mathbb{R}^{m\times m}$ are known matrices. Thus, the Kalman filter algorithm is:

$$\hat{x}_{k|k-1} = A_{k-1}\hat{x}_{k-1|k-1} + B_{k-1}u_{k-1}, \tag{3}$$
$$P_{k|k-1} = A_{k-1}P_{k-1|k-1}A_{k-1}^T + D_{k-1}, \tag{4}$$
$$G_k = P_{k|k-1}C_k^T\left(C_kP_{k|k-1}C_k^T + M_k\right)^{-1}, \tag{5}$$
$$\hat{x}_{k|k} = \hat{x}_{k|k-1} + G_k(y_k - C_k\hat{x}_{k|k-1}), \tag{6}$$
$$P_{k|k} = (I_{n\times n} - G_kC_k)\,P_{k|k-1}, \tag{7}$$

where $\hat{x}_{k-1|k-1}$ is the estimation for x_{k-1} at instant $k-1$, $\hat{x}_{k|k-1}$ is the prediction for state x_k at instant k and $\hat{x}_{k|k}$ is the corrected estimation for x_k at instant k. Similarly, $P_{k-1|k-1}$ is the estimation for the error variance at instant $k-1$, $P_{k|k-1}$ is the prediction for error variance at instant k and $P_{k|k}$ is the corrected estimation for the error variance at instant k. In both cases, the corrections of $\hat{x}_{k|k}$ and $P_{k|k}$ are carried out through the Kalman gain, namely, G_k.

B. REGULATION THEORY

Let the nonlinear plant be:

$$\dot{x}(t) = f(x(t), w(t), u(t)), \tag{8}$$
$$y(t) = h(x(t)), \tag{9}$$
$$\dot{w}(t) = s(w(t)), \tag{10}$$
$$y_{ref}(t) = q(w(t)), \tag{11}$$

where $x(t) \in \mathbb{R}^n$ is the vector state of the plant, $u(t) \in \mathbb{R}^p$ is the input vector of the plant, and $y(t) \in \mathbb{R}^m$ is the output vector of the plant, $w(t) \in \mathbb{R}^r$ is the state vector of and external signal generator, named exosystem, and $y_{ref} \in \mathbb{R}^m$ is the vector of reference signals. It is assumed that $f(\cdot,\cdot,\cdot)$, $h(\cdot)$, $s(\cdot)$ and $q(\cdot)$ are sufficiently smooth functions, i.e., they are assumed to be C^k functions for some large k of their arguments, fulfilling $f(0,0,0) = 0$, $h(0) = 0$, $s(0) = 0$ and $q(0) = 0$ [4], [5].

On this basis, the nonlinear regulation problem is defined as the problem of finding a control law $u(t)$ such that $y(t)$ asymptotically tends to $y_{ref}(t)$, even in the presence of external disturbances, where

$$u(t) = K(x(t) - \pi(w(t))) + \gamma(w(t)), \tag{12}$$

with K as the stabilizer gain, $\pi(w(t))$ as the steady-state manifold, which becomes invariant through the steady-state input $\gamma(w(t))$. The following theorem summarizes the existence conditions of (12).

Theorem 2.1: Suppose:

A1$_{nl}$) *there exists K such that the origin of $\dot{x}(t) = f(x(t), 0, Kx(t))$ is asymptotically stable,*

A2$_{nl}$) *there exist $x_{ss}(t) = \pi(w(t))$, $u_{ss}(t) = \gamma(w(t))$, fulfilling*:

$$\frac{\partial \pi(w(t))}{\partial w(t)}s(w(t)) = f(\pi(w(t)), w(t), \gamma(w(t))), \tag{13}$$

$$h(\pi(w(t))) = q(w(t)), \tag{14}$$

where (13)-(14) are known as the Francis-Byrnes-Isidori (FBI) equations, with $\pi(0) = 0$, *and* $\gamma(0) = 0$.

Then, the control law (12) solves the nonlinear regulation problem defined by (8)-(11).

Proof: Please refer to [5] for a thorough analysis of the nonlinear regulation problem. □

Obviously, the linear regulation problem arises directly after linearizing (8)-(12) around the origin, resulting:

$$\dot{x}(t) = Ax(t) + P_d w(t) + Bu(t), \tag{15}$$
$$y(t) = Cx(t), \tag{16}$$
$$\dot{w}(t) = Sw(t), \tag{17}$$
$$y_{ref}(t) = Qw(t), \text{ with} \tag{18}$$
$$u(t) = K(x(t) - \Pi w(t)) + \Gamma w(t), \tag{19}$$

where $A = \frac{\partial f}{\partial x}, B = \frac{\partial f}{\partial u}, P_d = \frac{\partial f}{\partial w}, C = \frac{\partial h}{\partial x}, S = \frac{\partial s}{\partial w}, Q = \frac{\partial q}{\partial w}$, with Π and Γ as the solution of the *Francis equations*.

The existence conditions for the linear regulator (19) are given in the following theorem.

Theorem 2.2: Suppose:

A1$_l$) *there exists* K *such that* $A + BK$ *is asymptotically stable,*

A2$_l$) *there exist* $x_{ss}(t) = \Pi w(t)$, $u_{ss}(t) = \Gamma w(t)$, *fulfilling*

$$\Pi S = A\Pi + B\Gamma + P_d, \tag{20}$$
$$C\Pi = Q, \tag{21}$$

where (20)-(21) are known as the Francis equations, with $\Pi \in \mathbb{R}^{n\times r}$, *and* $\Gamma \in \mathbb{R}^{p\times r}$.

Then, the control law (19) solves the linear regulation problem defined by (15)-(18).

Proof: Please refer to [6] for a thorough analysis of the linear regulation problem. □

Notice that in [13], both techniques have already been blended into a control scheme to achieve the tracking/rejecting of random signals. However, the main drawback of such an approach is that the explicit mathematical model of the exosystem is required to apply the regulation presented there.

C. CONTINUOUS-TIME POLYNOMIALS AS CONTINUOUS-TIME LINEAR SYSTEMS

Theorem 2.3: The signal $\psi(t)$ *defined as the polynomial*

$$\psi(t) = \alpha_\rho t^\rho + \alpha_{\rho-1} t^{\rho-1} + \ldots + \alpha_1 t + \alpha_0, \tag{22}$$

with the integer $\rho \geq 0$, *can be exactly described by the output,* $y_{ref}(t)$, *of the linear system*

$$\dot{w}(t) = S_c w(t), \tag{23}$$
$$y_{ref}(t) = Q_c w(t), \tag{24}$$

where

$$S_c = \begin{bmatrix} 0_{[\rho,1]} & I_{[\rho,\rho]} \\ 0 & 0_{[1,\rho]} \end{bmatrix}, \tag{25}$$

$$Q_c = \begin{bmatrix} 1 & 0_{[1,\rho]} \end{bmatrix}, \text{ and} \tag{26}$$
$$w(0) = \begin{bmatrix} \alpha_0 & \alpha_1 & 2!\alpha_2 & \ldots & \rho!\alpha_\rho \end{bmatrix}^T, \tag{27}$$

with $w(t) \in \mathbb{R}^{\rho+1}$ *as the state vector of the linear system (23)-(24),* $w(0) \in \mathbb{R}^{\rho+1}$ *as the vector of initial conditions for such a system,* $I_{[\rho,\rho]}$ *as the identity matrix of dimension* $\rho \times \rho$, *and* $0_{[1,\rho]}$ *as the row vector of zeros of dimension* $1 \times \rho$.

Proof: Consider that the signal $\psi(t)$ is replicated by the first state of the linear system (23)-(24), namely,

$$\psi(t) = \alpha_\rho t^\rho + \ldots + \alpha_1 t + \alpha_0 = w_1(t). \tag{28}$$

Then, the ρ remaining states of such a linear system can be defined by the successive time derivatives of $w_1(t)$, specifically:

$$\begin{aligned} \dot{w}_1(t) &= \rho\alpha_\rho t^{\rho-1} + \ldots + \alpha_1 = w_2(t), \\ &\vdots \\ \dot{w}_\rho(t) &= \rho!\alpha_\rho = w_{\rho+1}(t), \\ \dot{w}_{\rho+1}(t) &= 0. \end{aligned} \tag{29}$$

Obviously, $w(0)$ is obtained by substituting $t = 0$ in (28) and (29). Finally, it can be readily concluded that the signal $\psi(t)$ is equal to the output $y_{ref}(t)$ of the linear system (23)-(24), for all $t \geq 0$, when the matrices S_c and Q_c have the form of (25), and (26), respectively, with the vector of initial condition $w(0)$ as (27). □

D. DISCRETIZATION OF DYNAMICAL SYSTEMS USING THE FORWARD EULER METHOD

Consider the continuous-time nonlinear system

$$\dot{x}(t) = f(x(t), u(t)), \tag{30}$$
$$y(t) = h(x(t)), \tag{31}$$

and the expression of the derivative

$$\frac{dx}{dt} = \lim_{\Delta t \to 0} \frac{x(t + \Delta t) - x(t)}{\Delta t}, \tag{32}$$

where $\dot{x}(t) = \frac{dx}{dt}$.

Now suppose that the sampling period is T, then the discrete-time is given by kT, where k the sampling instant, with $k = 0, 1, 2, \ldots$. So, from (32), one gets:

$$\frac{dx}{dt} \approx \frac{x(t + T) - x(t)}{T}. \tag{33}$$

Thus, according to the forward Euler method, the discretization of (30)-(31) at $t = kT$ is readily obtained when (30) is substituted in (33). i.e.,

$$x((k+1)T) = x(kT) + T \cdot f(x(kT), u(kT)), \tag{34}$$
$$y(kT) = h(x(kT)). \tag{35}$$

For the sake of space, in the present work, the notation with sub-indexes is preferred over the one with arguments. Therefore, (34)-(35), can be rewritten as:

$$x_{k+1} = x_k + T \cdot f(x_k, u_k), \tag{36}$$

$$y_k = h(x_k). \tag{37}$$

In the same way, the Euler discretization of the continuous-time linear system

$$\dot{x}(t) = Ax(t) + Bu(t), \tag{38}$$
$$y(t) = Cx(t), \tag{39}$$

is

$$x_{k+1} = A_d x_k + B_d u_k, \tag{40}$$
$$y_k = C_d x_k, \tag{41}$$

where $A_d = I + T \cdot A$, $B_d = T \cdot B$, and $C_d = C$, with I as the identity matrix of adequate dimension [14].

E. PROBLEM FORMULATION

Consider the scenario where m reference signals must be imposed upon m outputs of a nonlinear system, while d disturbance signals have to be rejected. Besides, the $m + d$ reference/disturbance signals are non-modeled but digitally measurable. Without loss of generally, such signals can be arranged as the vector $\Psi(t) \in \mathbb{R}^{m+d}$, i.e.,

$$\Psi(t) = \begin{bmatrix} \Psi_{ref}(t) \\ \Psi_{dis}(t) \end{bmatrix}, \tag{42}$$

where $\Psi_{ref}(t) \in \mathbb{R}^m$ is the vector of m reference signals, and $\Psi_{dis}(t) \in \mathbb{R}^d$ is the vector of d reference signals. At this point, the nonlinear regulation problem can be defined as

$$\dot{x}(t) = f(x(t), \Psi_{dis}(t), u(t)), \tag{43}$$
$$y(t) = h(x(t)), \tag{44}$$
$$y_{ref}(t) = \Psi_{ref}(t). \tag{45}$$

Thus the main contribution of the present work is to design a Kalman filter not only to estimate the reference/disturbance signals, but to serve as a suitable model (exosystem) for such signals, with the aim that the regulation equations can be proposed. A graphical description of the control scheme is depicted in Fig. 1.

III. MAIN RESULT

A. A KALMAN FILTER USED TO ESTIMATE A SINGLE NON-MODELED NOISY POLYNOMIAL SIGNAL

As mentioned in section II-C, any continuous-time signal whose behavior is described as a continuous-time polynomial of degree ρ can be generated through the output of a continuous-time linear system of dimension $\rho + 1$. Thus, if such a signal is measured through a digital device, then a discrete-time signal is obtained. However, in most cases, the time-discrete signal will be tainted with measurement noise. Therefore, the Kalman filter (KF) is a natural alternative not even to estimate and filter the discrete-time signal, but also to provide a dynamic model of such a signal.

Clearly, before using the KF to estimate a non-modeled signal, the linear system assumed to generate such a continuous-time polynomial signal must be discretized using the results depicted in Section II-D. Thus, any discrete-time signal ψ_k generated by a polynomial of degree ρ can be replicated by the output of the following discrete-time linear system:

$$w_{k+1} = S_{blk} w_k, \tag{46}$$
$$\psi_k = Q_{blk} w_k, \tag{47}$$

where T is the sampling period, k is the sampling instant, $w_k \in \mathbb{R}^{\rho+1}$, $\psi_k \in \mathbb{R}$, $S_{blk} = I_{[\rho+1,\rho+1]} + T \cdot S_c$, and $Q_{blk} = Q_c$, with S_c and Q_c as in (25), and (26), respectively. Now, suppose that the system (46)-(47) is contaminated by dynamic and measurement noises with zero mean and variances D_{blk} and M_{blk}, respectively. Then, the resulting stochastic discrete-time linear system is:

$$w_{k+1} = S_{blk} w_k + \xi_k, \tag{48}$$
$$\psi_k = Q_{blk} w_k + \eta_k, \tag{49}$$

where $\xi_k \in \mathbb{R}^{\rho+1}$ is the dynamic noise with zero mean and variance $D_{blk} \in \mathbb{R}^{(\rho+1)\times(\rho+1)}$, $\eta_k \in \mathbb{R}$ is the measurement noise with zero mean and variance $M_{blk} \in \mathbb{R}$, and with S_{blk}, and Q_{blk} as before. Thus, the KF algorithm for (48)-(49) is:

$$\hat{w}_{k|k-1} = S_{blk} \hat{w}_{k-1|k-1}, \tag{50}$$
$$P_{k|k-1} = S_{blk} P_{k-1|k-1} S_{blk}^T + D_{blk}, \tag{51}$$
$$G_k = P_{k|k-1} Q_{blk}^T \left(Q_{blk} P_{k|k-1} Q_{blk}^T + M_{blk} \right)^{-1}, \tag{52}$$
$$\hat{w}_{k|k} = \hat{w}_{k|k-1} + G_k (\psi_k - Q_{blk} \hat{w}_{k|k-1}), \tag{53}$$
$$P_{k|k} = \left(I_{[\rho+1,\rho+1]} - G_k Q_{blk} \right) P_{k|k-1}, \tag{54}$$

because S_{blk}, Q_{blk}, D_{blk}, and M_{blk} are constants.

B. A KALMAN FILTER USED TO ESTIMATE A VECTOR OF NON-MODELED NOISY POLYNOMIAL SIGNALS

Consider the set of $\tilde{m}$ discrete-time polynomial signals, namely, $\psi_{1,k}, \ldots, \psi_{\tilde{m},k}$, generated by polynomials of degree $\rho_1, \ldots, \rho_{\tilde{m}}$, respectively, and the vector $\Psi_k = [\psi_{1,k} \ldots \psi_{\tilde{m},k}]^T$. Then, from the discussion carried out in the previous section, it can be readily deduced that Ψ_k can be estimated by the output of an overall KF of diagonal form, constructed by $\tilde{m}$ independent KFs, where each of the particular blocks might have different dimensions depending on the values $\rho_1, \ldots, \rho_{\tilde{m}}$. The complete stochastic linear system is

$$w_{k+1} = S w_k + \xi_k, \tag{55}$$
$$\Psi_k = Q w_k + \eta_k, \tag{56}$$

and the KF algorithm for (55)-(56) is:

$$\hat{w}_{k|k-1} = S \hat{w}_{k-1|k-1}, \tag{57}$$
$$P_{k|k-1} = S P_{k-1|k-1} S^T + D, \tag{58}$$
$$G_k = P_{k|k-1} Q^T \left(Q P_{k|k-1} Q^T + M \right)^{-1}, \tag{59}$$
$$\hat{w}_{k|k} = \hat{w}_{k|k-1} + G_k (\Psi_k - Q \hat{w}_{k|k-1}), \tag{60}$$
$$P_{k|k} = (I - G_k Q) P_{k|k-1}, \tag{61}$$

where $w_k, \xi_k \in \mathbb{R}^{\rho_1+\ldots+\rho_{\tilde{m}}+\tilde{m}}$, $\Psi_k, \eta_k \in \mathbb{R}^{\tilde{m}}$, $S = diag(S_{blk,1}, \ldots, S_{blk,\tilde{m}})$, $Q = diag(Q_{blk,1}, \ldots, Q_{blk,\tilde{m}})$, $D =$

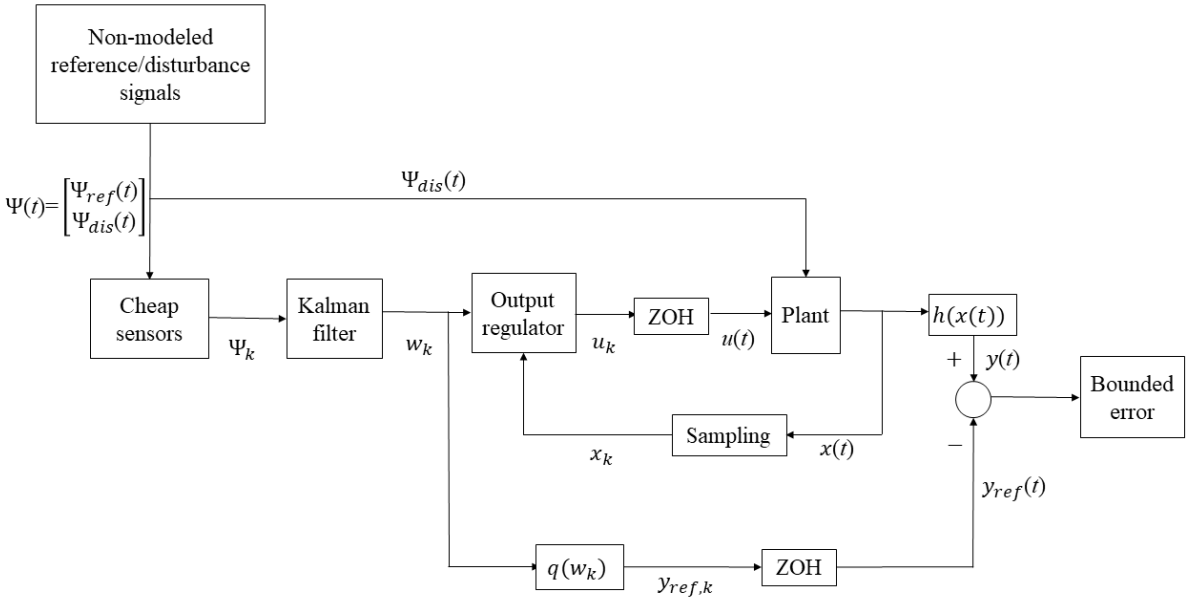

FIGURE 1. The control scheme, where $\Psi(t) = [\,\Psi_{ref}^T(t)\ \Psi_{dis}^T(t)\,]^T$ is formed by the vectors $\Psi_{ref} \in \mathbb{R}^m$, and $\Psi_{dis} \in \mathbb{R}^d$, where the former includes the non-modeled reference signals, while the latter includes the non-modeled disturbance signals, both contaminated with noise because of the measuring process. Besides, "ZOH" stands for "Zero order hold."

$diag(D_{blk,1}, \ldots, D_{blk,\tilde{m}})$, and $M = diag(M_{blk,1}, \ldots, M_{blk,\tilde{m}})$, with $S_{blk,1}, \ldots, S_{blk,\tilde{m}}, Q_{blk,1}, \ldots, Q_{blk,\tilde{m}}, D_{blk,1}, \ldots, D_{blk,\tilde{m}}$, and $M_{blk,1}, \ldots, M_{blk,\tilde{m}}$ as S_{blk}, Q_{blk}, D_{blk} and M_{blk}, respectively, but considering the adequate values $\rho_1, \ldots, \rho_{\tilde{m}}$, and with I as the identity matrix of dimension $\rho_1 + \ldots + \rho_{\tilde{m}} + \tilde{m}$.

C. THE OUTPUT REGULATOR WHEN THE EXOSYSTEM IS A KALMAN FILTER

Thus, according to Section II-E, suppose that Ψ_k is the vector with the reference/perturbation signals obtained by sampling the vector (42), i.e.,

$$\Psi_k = \begin{bmatrix} \Psi_{ref,k} \\ \Psi_{dis,k} \end{bmatrix}. \tag{62}$$

Then, the linear stochastic system that can be used as the mathematical model for such signals and as the exosystem for the regulation problem has the form of (55)-(56), which can be estimated by the KF (57)-(61), where $\tilde{m} = m + d$, $w_k, \xi_k \in \mathbb{R}^{\rho_1+\ldots+\rho_{\tilde{m}}+\tilde{m}}$, $\Psi_k, \eta_k \in \mathbb{R}^{\tilde{m}}$, $S = diag(S_{blk,1}, \ldots, S_{blk,\tilde{m}})$, $Q = [Q_{ref},\ 0_{[m,\rho_{m+1}+\ldots+\rho_{\tilde{m}}]}]$, $D = diag(D_{blk,1}, \ldots, D_{blk,\tilde{m}})$, and $M = diag(M_{blk,1}, \ldots, M_{blk,\tilde{m}})$, with $Q_{ref} = diag(Q_{blk,1}, \ldots, Q_{blk,m})$, $S_{blk,1}, \ldots, S_{blk,\tilde{m}}$, $Q_{blk,1}, \ldots, Q_{blk,m}, D_{blk,1}, \ldots, D_{blk,\tilde{m}}$, and $M_{blk,1}, \ldots, M_{blk,\tilde{m}}$ as S_{blk}, Q_{blk}, D_{blk} and M_{blk}, respectively, but considering the adequate values $\rho_1, \ldots, \rho_{\tilde{m}}$. furthermore, $0_{[m,\rho_{m+1}+\ldots+\rho_{\tilde{m}}]}$ is the zero matrix of dimension $m \times (\rho_{m+1} + \ldots + \rho_{\tilde{m}})$.

At this point, the discrete-time nonlinear regulation problem, when the reference/disturbance signals are non-modeled and contaminated with white noises, can be defined as

$$x_{k+1} = f_d(x_k, \Psi_{dis,k}, u_k), \tag{63}$$
$$y_k = h_d(x_k), \tag{64}$$
$$w_{k+1} = Sw_k + \xi_k, \tag{65}$$
$$\Psi_{ref,k} = Qw_k + \eta_k, \text{ with} \tag{66}$$
$$u_k = K(x_k - \pi(w_k)) + \gamma(w_k). \tag{67}$$

Notice that the KF algorithm requires the past values of its estimations and covariance matrix. For that reason, it can be easily observed that the KF filter algorithm is, in fact, a nonlinear discrete-time system of dimension $\tilde{m} + \tilde{m}^2$.

Therefore, to keep the approach as practical as possible, the regulation problem will be stated as its linear version, i.e.,

$$x_{k+1} = Ax_k + P_d w_k + Bu_k, \tag{68}$$
$$y_k = Cx_k, \tag{69}$$
$$w_{k+1} = Sw_k, \tag{70}$$
$$y_{ref,k} = Q_k, \text{ with} \tag{71}$$
$$u_k = K(x_k - \Pi w_k) + \Gamma w_k, \tag{72}$$

where $A = \frac{\partial f_d}{\partial x}$, $B = \frac{\partial f_d}{\partial u}$, $P_d = \frac{\partial f_d}{\partial \Phi_{dis}}$, $C = \frac{\partial h_d}{\partial x}$, with S, and Q as above and Π, and Γ as the solution of the Francis equations (20)-(21).

IV. NUMERICAL EXPERIMENTS

A. THE MODEL OF THE QUADROTOR

In this section, the previous results are applied to the mathematical model of the quadrotor analyzed in [15], which scheme is depicted in Fig. 2 and whose dynamics are described in the following equations:

$$\dot{x}(t) = f(x(t), u(t)), \tag{73}$$
$$y(t) = h(x(t)), \tag{74}$$

where $x(t) = [x_1(t) \dots x_{12}(t)]^T$, $u(t) = [u_1(t) \ \dots \ u_4(t)]^T$, and

$$\dot{x}_1(t) = x_2(t), \tag{75}$$
$$\dot{x}_2(t) = (\sin(x_{11}(t))\sin(x_7(t)) + \cos(x_{11}(t)) \times \sin(x_9(t))\cos(x_7(t)))\frac{\beta_1(t)}{m}, \tag{76}$$
$$\dot{x}_3(t) = x_4(t), \tag{77}$$
$$\dot{x}_4(t) = (-\cos(x_{11}(t))\sin(x_7(t)) + \sin(x_{11}(t)) \times \sin(x_9(t))\cos(x_7(t)))\frac{\beta_1(t)}{m}, \tag{78}$$
$$\dot{x}_5(t) = x_6(t), \tag{79}$$
$$\dot{x}_6(t) = -g + (\cos(x_9(t))\cos(x_7(t))\frac{\beta_1(t)}{m}, \tag{80}$$
$$\dot{x}_7(t) = x_8(t), \tag{81}$$
$$\dot{x}_8(t) = x_{10}(t)x_{12}(t)\frac{I_{yy} - I_{zz}}{I_{xx}} - \frac{J_{tp}}{I_{xx}}x_{10}(t)\Omega(t) + \frac{l\beta_2(t)}{I_{xx}}, \tag{82}$$
$$\dot{x}_9(t) = x_{10}(t), \tag{83}$$
$$\dot{x}_{10}(t) = x_8(t)x_{12}(t)\frac{I_{zz} - I_{xx}}{I_{yy}} + \frac{J_{tp}}{I_{yy}}x_8(t)\Omega(t) + \frac{l\beta_3(t)}{I_{yy}}, \tag{84}$$
$$\dot{x}_{11}(t) = x_{12}(t), \tag{85}$$
$$\dot{x}_{12}(t) = x_8(t)x_{10}(t)\frac{I_{xx} - I_{yy}}{I_{zz}} + \frac{\beta_4(t)}{I_{zz}}, \tag{86}$$

with $\beta_1(t)$ as the force responsible for throttle movement, $\beta_2(t)$ as the torque responsible for roll movement, $\beta_3(t)$ as the torque responsible for pitch movement, and $\beta_4(t)$ as the torque responsible for yaw movement, given by

$$\beta_1(t) = b(u_1(t)^2 + u_2(t)^2 + u_3(t)^2 + u_4(t)^2), \tag{87}$$
$$\beta_2(t) = b(u_4(t)^2 + u_3(t)^2 - u_1(t)^2 - u_2(t)^2), \tag{88}$$
$$\beta_3(t) = b(u_2(t)^2 + u_3(t)^2 - u_1(t)^2 - u_4(t)^2), \tag{89}$$
$$\beta_4(t) = d(u_1(t)^2 + u_3(t)^2 - u_2(t)^2 - u_4(t)^2), \tag{90}$$
$$\Omega(t) = u_1(t) - u_2(t) + u_3(t) - u_4(t), \tag{91}$$

and

$$h(x(t)) = C_f x(t), \ \text{with } C_f = I_{[12\times 12]}. \tag{92}$$

Notice that $u_1(t)$, $u_2(t)$, $u_3(t)$ and $u_4(t)$ are the frequencies of rotors 1, 2, 3 and 4, respectively, i.e., they are the implicit control inputs and they are given in rad/s. The variables $x_1(t)$, $x_3(t)$ and $x_5(t)$ represent the linear displacements along the earth fixed axes X_e, Y_e and Z_e, respectively, and they are in meters. On the other hand, the variables $x_7(t)$, $x_9(t)$ and $x_{11}(t)$ describe the angular displacements around the body axes X_b, Y_b and Z_b, respectively, and they are in radians. The remaining state variables describe the linear and angular velocities, and they can be easily deduced from (73)-(92). The considered values for the parameters appear in Table 1. With

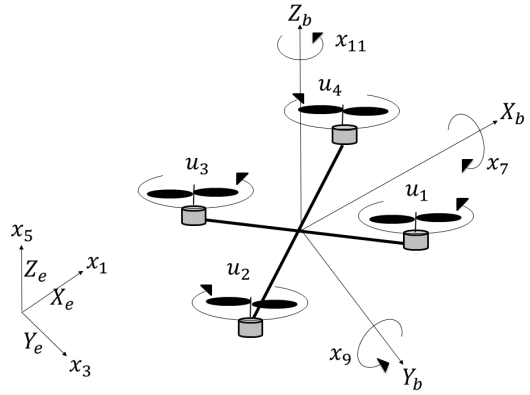

FIGURE 2. Diagram of the quadrotor.

TABLE 1. Parameters of the quadrotor.

Description	Symbol	Value	Units
Thrust factor	b	54.2×10^{-6}	$N \cdot s^2$
Drag factor	d	1.1×10^{-6}	$N \cdot m \cdot s^2$
Distance from the center of the quadrotor to the center of the rotors	l	0.24	m
Mass	m	1	kg
Gravity	g	9.81	m/s^2
Total moment of inertia for the rotors	J_{tp}	104×10^{-6}	$N \cdot m \cdot s^2$
Moment of inertia respect to axe x	Ixx	8.1×10^{-3}	$N \cdot m \cdot s^2$
Moment of inertia respect to axe y	Iyy	8.1×10^{-3}	$N \cdot m \cdot s^2$
Moment of inertia respect to axe z	Izz	14.2×10^{-3}	$N \cdot m \cdot s^2$

such parameters, the quadrotor remains in hover position when $u_1 = u_2 = u_3 = u_4 = 212.72 rad/s$.

The considered sampling time is $T = 0.02s$. Therefore, the nonlinear discrete-time model in the form of (36)-(37) can be readily obtained. The matrices forming the discrete-time linear system (40)-(41) can be found in Appendix A. Note that the quadcopter's model used in this work does not consider the ground effect, so the altitude is not relevant for the linearization process. Moreover, the analysis of the quadcopter's dynamics indicates that only the horizontal position can be an equilibrium point. For that reason, the origin is chosen as the linearization point.

Now suppose that non-modeled but measurable signals need to be tracked by each one of the four independent degrees of freedom of the quadrotor, namely the reference signals

$$y_{ref}(t) = \begin{bmatrix} \psi_1(t) \\ \psi_2(t) \\ \psi_3(t) \\ \psi_4(t) \end{bmatrix}, \tag{93}$$

must be imposed on the outputs

$$y(t) = \begin{bmatrix} x_1(t) \\ x_3(t) \\ x_5(t) \\ x_{11}(t) \end{bmatrix}, \tag{94}$$

respectively. Thus, the matrix C that must be considered during the solution of the regulation equations (20)-(21) has four rows and twelve columns, and it is also given in the Appendix A.

Besides, suppose $P_d = 0$ because there are no disturbance signals affecting the quadrotor. So, according to the discussion carried on in Section III, one gets $m = 4$, $d = 0$, and $\tilde{m} = 4$.

Under these assumptions, in the following sections the regulator problem defined by (68)-(72) is solved considering Kalman filters of different order. In each case, the control law (72) is applied on the nonlinear system (73)-(92) to illustrate the validity of the proposed approach.

At this point, it is important to mention that the matrix K considered in the examples is computed by means of the linear quadratic regulator theory [16] through the function *lqr* of Matlab©, such a gain is given in the Appendix A.

B. EXOSYSTEM CONSTRUCTED FROM KALMAN FILTERS OF 3rd ORDER

In this section, the non-modeled signals: $\psi_1(t) = sin(\frac{\pi}{20}t) + sin((\frac{\pi}{20}+0.1)t)$, $\psi_2(t) = cos(\frac{\pi}{20}t)$, $\psi_3(t) = 5$, and $\psi_4(t) = 0$, are approximated by polynomials of 2nd degree, i.e., $\rho_i = 2$, for $i = 1, \ldots, 4$. Therefore, per the analysis presented in Section II, the corresponding Kalman filters are of 3rd order, and the order of the overall exosystem is 12, because, as explained in the previous section, in this example, the matrix S is a diagonal matrix constructed by four blocks of the form:

$$S_{blk,i} = I + T \cdot \begin{bmatrix} 0 & 1 & 0 \\ 0 & 0 & 1 \\ 0 & 0 & 0 \end{bmatrix} = \begin{bmatrix} 1 & 0.02 & 0 \\ 0 & 1 & 0.02 \\ 0 & 0 & 1 \end{bmatrix}, \qquad (95)$$

while the matrix Q is also a diagonal matrix shaped by 4 blocks of the form:

$$Q_{blk,i} = \begin{bmatrix} 1 & 0 & 0 \end{bmatrix}, \qquad (96)$$

for $i = 1, \ldots, 4$. Notice that due to the nonexistence of disturbances, and by the dimensions of the plant and the exosystem, in this case, $Pd = 0_{[12,12]}$. Besides, it is considered that the noises induced by the sensors used to measure the reference signals have a standard deviation equal to 0.1. Therefore, the matrix M is:

$$M = (0.1)^2 I_{4\times 4} = 0.01 I_{[4\times 4]}. \qquad (97)$$

On the other hand, the dynamical noises are neglected. As a consequence, in this work, the matrix D is:

$$Q = 1 \times 10^{-12} I_{[12\times 12]}. \qquad (98)$$

The rest of the matrices, i.e., A, B, C, S and Q considered during the solution of the Francis equations (20)-(21), and also the solutions of such equations, namely, Π and Γ can be found in Appendix A.

The results of applying the regulator (72) on the nonlinear systems (73)-(92) are given from Fig. 3 to Fig. 9.

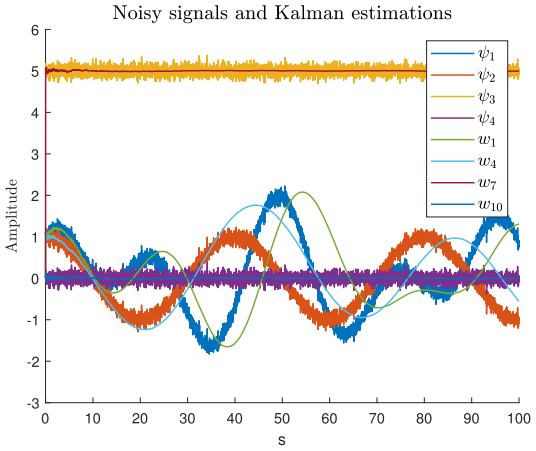

FIGURE 3. Measured signals and the estimations through the exosystem when the Kalman filters are of order 3.

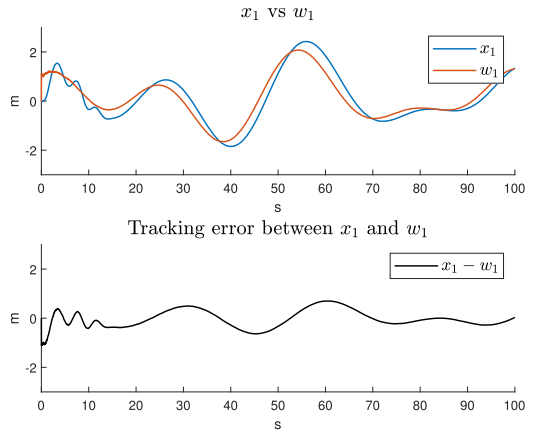

FIGURE 4. Comparison between the first state of the quadrotor and the first state of the exosystem when the Kalman filters are of order 3.

From Fig. 3, it can be observed that the Kalman estimations diverge from the actual signals $\psi_1(t)$ and $\psi_2(t)$ once the quadratic behavior is reached. This is due to the consideration of polynomials of second degree to approximate the reference signals. Moreover, this is unfortunate because such estimations become the reference signals to be tracked by the regulator.

Figs. 4 to 7 are included to show the performance of the regulator. Observe how the constant references are tracked relatively fine, while the tracking of the references that change over time is not exact. This is because only the linear part of the Kalman filters has been considered during the design of the regulator. However, if the estimations were more precise, the overall tracking errors may be more acceptable. Thus, the poor estimates plus the tracking errors might be inconvenient in many applications. For that reason, in the next section, the estimations are improved by considering polynomials of higher order.

In order to provide more conclusive results, the control signals are given in Figs. 8 and 9. From those figures, it can be concluded that the rotors are working within their valid ranges.

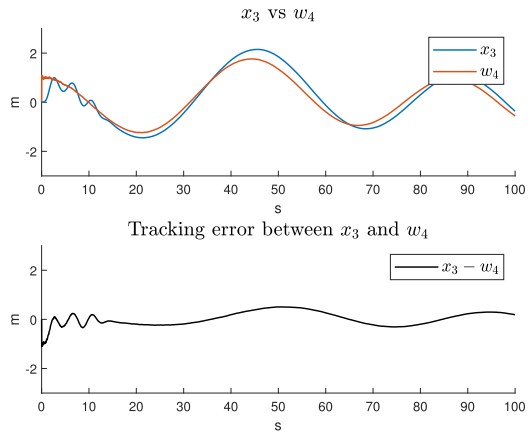

FIGURE 5. Comparison between the third state of the quadrotor and the fourth state of the exosystem when the Kalman filters are of order 3.

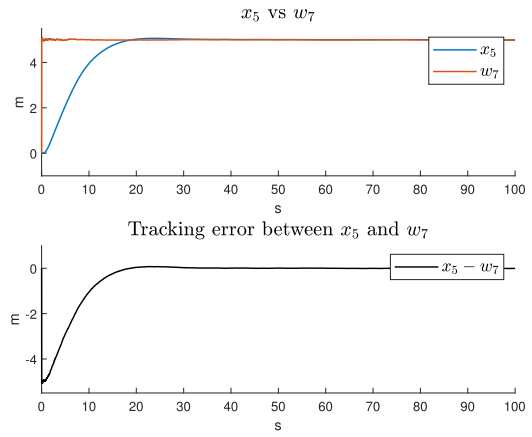

FIGURE 6. Comparison between the fifth state of the quadrotor and the seventh state of the exosystem when the Kalman filters are of order 3.

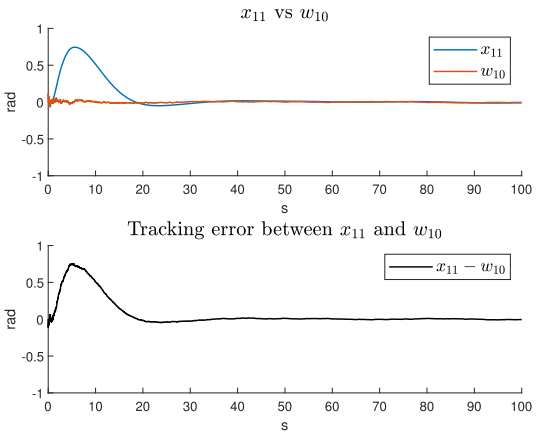

FIGURE 7. Comparison between the eleventh state of the quadrotor and the tenth state of the exosystem when the Kalman filters are of order 3.

C. EXOSYSTEM CONSTRUCTED FROM KALMAN FILTERS OF 7th ORDER

Now, the non-modeled signals are approximated by polynomials of 6th degree. Therefore, the associated Kalman filters are of order 7. Thus, the overall exosystem has order 28, because, now, the matrix S is a diagonal matrix constructed

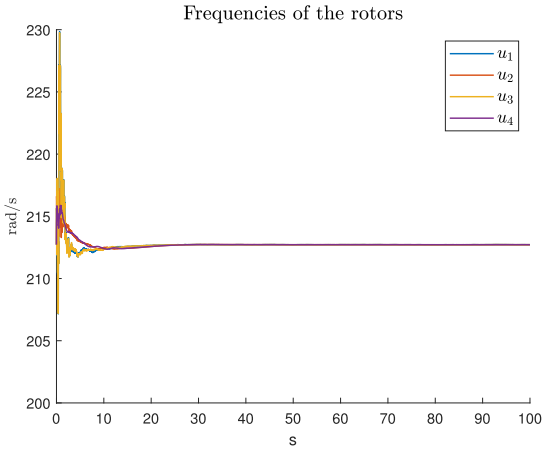

FIGURE 8. Control signals when the exosystem is constructed by Kalman filters are of order 3.

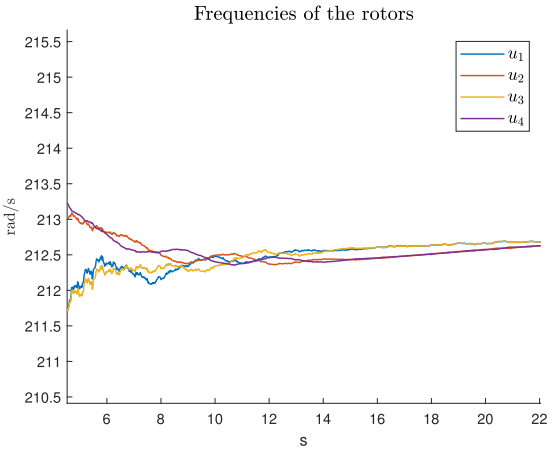

FIGURE 9. Control signals (zoomed) when the exosystem is constructed by Kalman filters are of order 3.

by four blocks of the form:

$$S_{blk,i} = \begin{bmatrix} 1 & T & 0 & 0 & 0 & 0 & 0 \\ 0 & 1 & T & 0 & 0 & 0 & 0 \\ 0 & 0 & 1 & T & 0 & 0 & 0 \\ 0 & 0 & 0 & 1 & T & 0 & 0 \\ 0 & 0 & 0 & 0 & 1 & T & 0 \\ 0 & 0 & 0 & 0 & 0 & 1 & T \\ 0 & 0 & 1 & 0 & 0 & 0 & 1 \end{bmatrix}, \tag{99}$$

with $T = 0.02s$, while the matrix Q is also a diagonal matrix shaped by 4 blocks of the form:

$$Q_{blk,i} = \begin{bmatrix} 1 & 0 & 0 & 0 & 0 & 0 & 0 \end{bmatrix}, \tag{100}$$

for $i = 1, \ldots, 4$. As before, no disturbances are considered, and by the dimensions of the plant and the exosystem, then in this example, $Pd = 0_{[12,28]}$. The overall matrices S and Q, and also the solutions of the Francis equations, Π and Γ, are given in the Appendix A. The results of applying the new regulator (72) appear in Figs. 10 to 16.

From Fig. 10, it can be observed that the Kalman estimations are very close to the actual signals $\psi_1(t)$ and $\psi_2(t)$ even

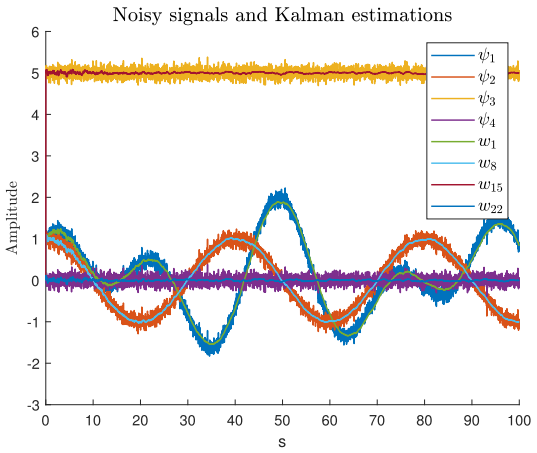

FIGURE 10. Measured signals and the estimations through the exosystem when the Kalman filters are of order 7.

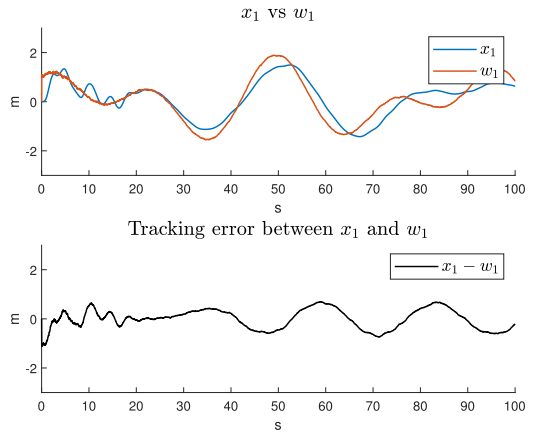

FIGURE 11. Comparison between the first state of the quadrotor and the first state of the exosystem when the Kalman filters are of order 7.

after the quadratic behavior is reached. This is due to the consideration of polynomials of sixth degree to approximate the reference signals.

The performance of the regulator can be deduced from Figs. 11 to 14. In this example, the constant references are still tracked relatively fine, while the tracking of the references that change over time remains not exact. However, the overall errors are notably better because now only the tracking errors are present.

The control signals for this numerical experiment are given in Figs. 15 and 16. Again, they range around their nominal values.

Remark 1: Note that the control design has been simplified by assuming that the states of the quadcopter and the rotor speeds are available. However, in a more realistic scenario, such data must be estimated. In that case, the application of the proposed approach would be similar to the one described in the examples.

D. EXOSYSTEM CONSTRUCTED FORM HIGH-GAIN OBSERVERS OF 2nd ORDER

To highlight the strengths and weaknesses of the proposed method, in this section, the exosystem is constructed using

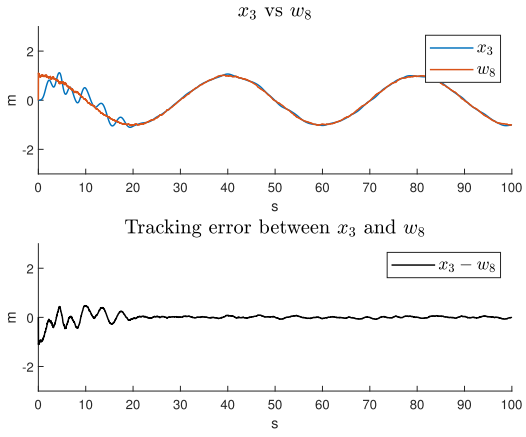

FIGURE 12. Comparison between the third state of the quadrotor and the eighth state of the exosystem when the Kalman filters are of order 7.

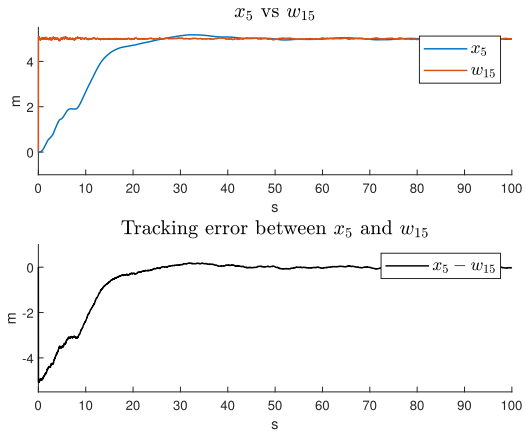

FIGURE 13. Comparison between the fifth state of the quadrotor and the 15th state of the exosystem when the Kalman filters are of order 7.

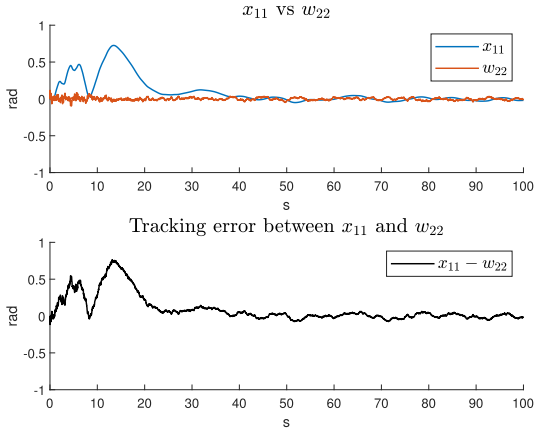

FIGURE 14. Comparison between the eleventh state of the quadrotor and the 22th state of the exosystem when the Kalman filters are of order 7.

HGOs as in [8] and [9]. For the sake of simplicity, each one of HGOs has dimension $\rho = 2$, and they are obtained considering $\alpha_1 = \alpha_2 = 1$, and $\epsilon = 0.02$. Therefore, the

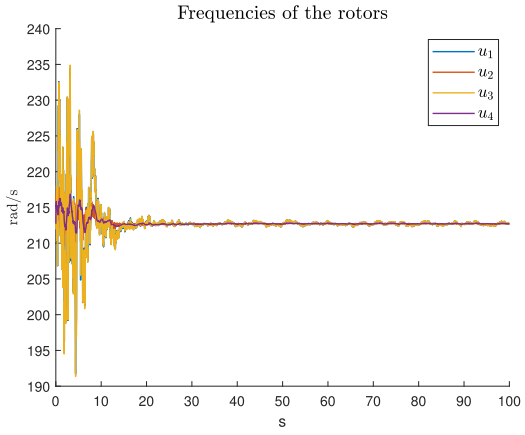

FIGURE 15. Control signals when the Kalman filters are of order 7.

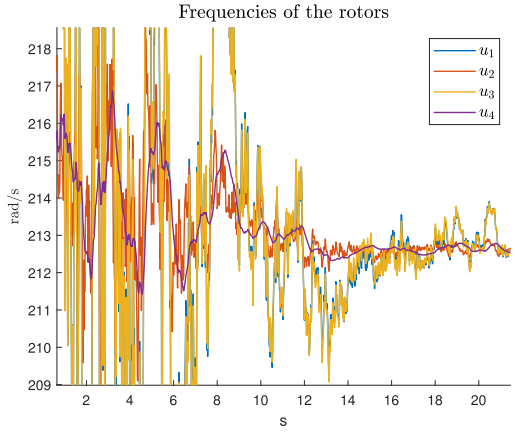

FIGURE 16. Control signals (zommed) when the exosystem is constructed by Kalman filters are of order 7.

corresponding block matrices, S, SH, and Q are:

$$S = \begin{bmatrix} -1 & \frac{1}{50} & 0 & 0 & 0 & 0 & 0 & 0 \\ -50 & 1 & 0 & 0 & 0 & 0 & 0 & 0 \\ 0 & 0 & -1 & \frac{1}{50} & 0 & 0 & 0 & 0 \\ 0 & 0 & -50 & 1 & 0 & 0 & 0 & 0 \\ 0 & 0 & 0 & 0 & -1 & \frac{1}{50} & 0 & 0 \\ 0 & 0 & 0 & 0 & -50 & 1 & 0 & 0 \\ 0 & 0 & 0 & 0 & 0 & 0 & -1 & \frac{1}{50} \\ 0 & 0 & 0 & 0 & 0 & 0 & -50 & 1 \end{bmatrix}, \tag{101}$$

$$S_H = \begin{bmatrix} 2 & 0 & 0 & 0 \\ 50 & 0 & 0 & 0 \\ 0 & 2 & 0 & 0 \\ 0 & 50 & 0 & 0 \\ 0 & 0 & 2 & 0 \\ 0 & 0 & 50 & 0 \\ 0 & 0 & 0 & 2 \\ 0 & 0 & 0 & 50 \end{bmatrix}, \tag{102}$$

and

$$Q = \begin{bmatrix} 1 & 0 & 0 & 0 & 0 & 0 & 0 & 0 \\ 0 & 0 & 1 & 0 & 0 & 0 & 0 & 0 \\ 0 & 0 & 0 & 0 & 1 & 0 & 0 & 0 \\ 0 & 0 & 0 & 0 & 0 & 0 & 1 & 0 \end{bmatrix}. \tag{103}$$

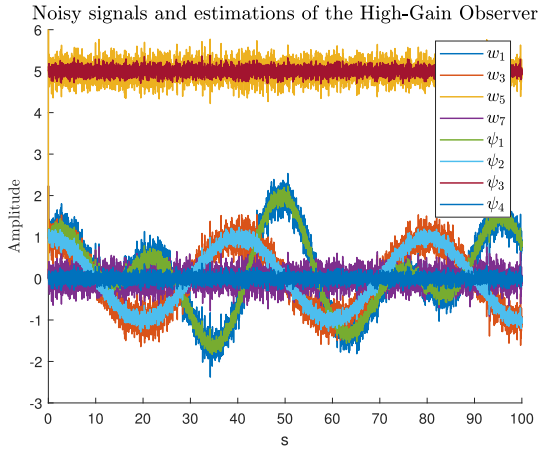

FIGURE 17. Measured signals and the estimations through the exosystem constructed by High-Gain Observes of order 2.

Thus, after solving the modified Francis equations derived in [8] and [9] with A, B, and C given in Appendix A, one gets:

$$\Pi = \begin{bmatrix} 1 & 0 & 0 & 0 & 0 & 0 & 0 & 0 \\ 0 & 1 & 0 & 0 & 0 & 0 & 0 & 0 \\ 0 & 0 & 1 & 0 & 0 & 0 & 0 & 0 \\ 0 & 0 & 0 & 1 & 0 & 0 & 0 & 0 \\ 0 & 0 & 0 & 0 & 1 & 0 & 0 & 0 \\ 0 & 0 & 0 & 0 & 0 & 1 & 0 & 0 \\ 0 & 0 & 0 & 0 & 0 & 0 & 0 & 0 \\ 0 & 0 & 0 & 0 & 0 & 0 & 0 & 0 \\ 0 & 0 & 0 & 0 & 0 & 0 & 0 & 0 \\ 0 & 0 & 0 & 0 & 0 & 0 & 0 & 0 \\ 0 & 0 & 0 & 0 & 0 & 0 & 1 & 0 \\ 0 & 0 & 0 & 0 & 0 & 0 & 0 & 1 \end{bmatrix}, \tag{104}$$

and

$$\Gamma = \begin{bmatrix} 0 & 0 & 0 & 0 & 0 & 0 & 0 & 0 \\ 0 & 0 & 0 & 0 & 0 & 0 & 0 & 0 \\ 0 & 0 & 0 & 0 & 0 & 0 & 0 & 0 \\ 0 & 0 & 0 & 0 & 0 & 0 & 0 & 0 \end{bmatrix}. \tag{105}$$

The stabilizer gain K, and the nonmodeled reference signals are the same considered in the previous examples. The estimations of the exosystem constructed on HGOs are depicted in Fig 17.

Remark 2: Note that the HGOs attempt to estimate the noisy nonmodeled signals as accurately as possible. In fact, if ρ is smaller, the estimations of the HGOs are even closer to the noisy signals. Consequently, a significant part of the undesirable noise is transmitted to the quadrotor through the regulator. In other words, the nonlinear system (73)-(92) becomes unstable by action of the regulator designed on HGOs.

As expected, the HGO-based regulator cannot be applied to the nonlinear plant, but it can be used on the linear approximation of the quadrotor. The simulation results are shown in Figs. 17 to 23.

Figs. 22 and 23 reveal the problem, which is that the control signals have high peaks and high frequencies that cause the

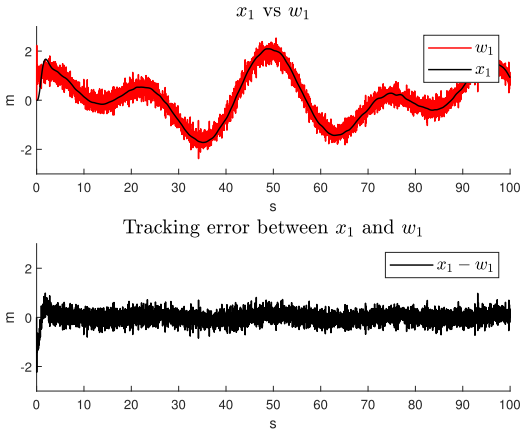

FIGURE 18. First state of the exosystem constructed by High-Gain Observers of order 2 compared with the first state of the linear approximation of the quadrotor.

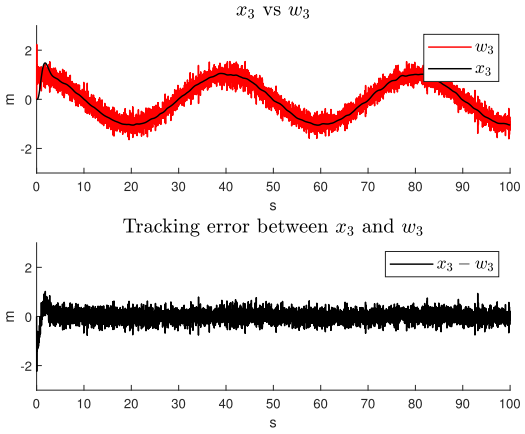

FIGURE 19. Third state of the linear approximation of the quadrotor compared with the third state of the exosystem constructed by High-Gain Observers of order 2.

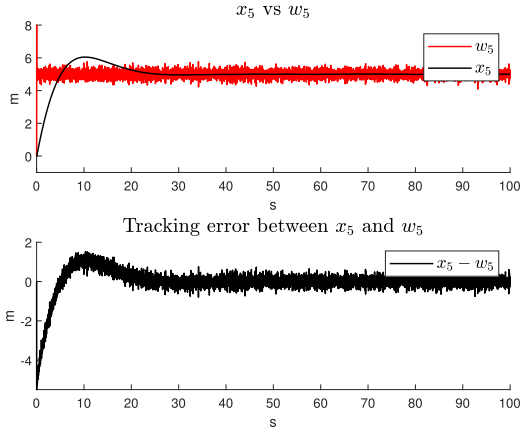

FIGURE 20. Fifth state of the exosystem constructed by High-Gain Observers of order 2 compared with the fifth state of the linear approximation of the quadrotor.

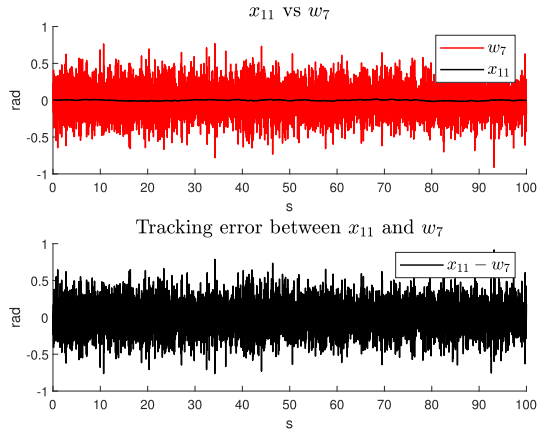

FIGURE 21. Eleventh state of the linear approximation of the quadrotor compared with the seventh state of the exosystem constructed by High-Gain Observers of order 2.

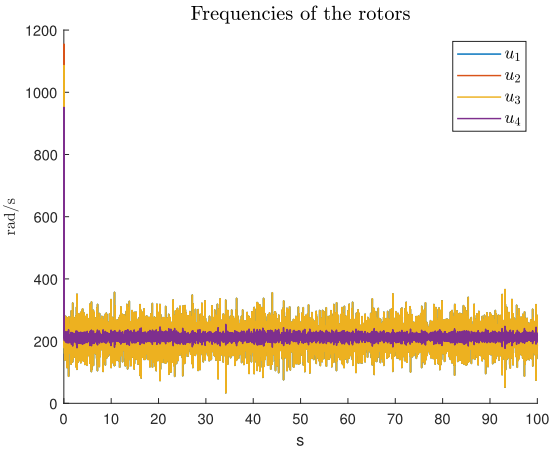

FIGURE 22. Control signals when the exosystem is constructed by High-Gain Observes of order 2.

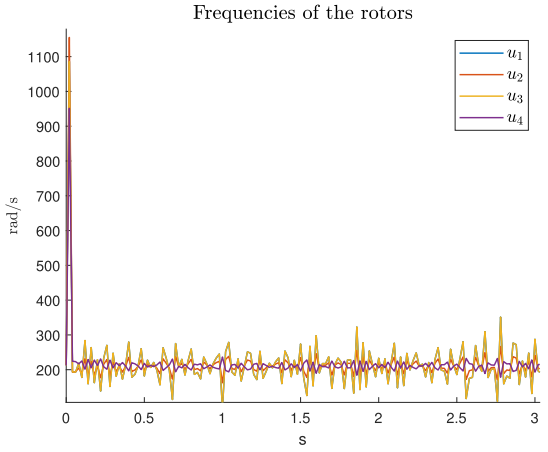

FIGURE 23. Control signals (zommed) when the exosystem is constructed by High-Gain Observes of order 2.

instability of the nonlinear plant. Another disadvantage may be the energy consumption.

A formal comparison of the complexity of the two approaches is left for future work, but at this point, it can be inferred that the HGO-based regulator does not require a high-dimensional exosystem to estimate the complex non-modeled signals, unlike the KF-based regulator. However, the HGO-based regulator needs a prior filtering process to deal with noisy signals regardless of their simplicity, whereas the

KF-based regulator does not require any additional filtering process.

V. CONCLUSION

An alternative based on the Kalman filter to applying the theory of linear regulation, even when the reference/disturbance signals are not modeled and are contaminated with noise when measured, has been presented. During the design of the regulator, only the linear part of the Kalman filter is considered, which allows the calculation of the controller to be carried out practically. Through a couple of examples, it has been shown that Kalman filters of higher order might help to obtain better estimations of the non-modeled and noisy signals. However, the overfitting problem can arise if the order of the Kalman filter is too high. Therefore, it is recommended to analyze each particular tracking problem carefully. The applications of the proposed approach range from recreational ones, such as a quadrotor tracking an object which moves on the floor or in the 3D space, to space and military ones, such as those related to the docking of space modules or intercepting flying objects. Finally, a sufficiently complex problem was analyzed to illustrate the validity of the approach, and a comparison with an HGO-based regulator was also provided.

APPENDIX A

After linearizing the discrete-time model of the quadrotor around the origin, and by considering the outputs to be regulated, the matrices A, B, and C to be used in the Francis equations (20)-(21) are:

$$A = \begin{bmatrix} 1 & 0.02 & 0 & 0 & 0 & 0 \\ 0 & 1 & 0 & 0 & 0 & 0 \\ 0 & 0 & 1 & 0.02 & 0 & 0 \\ 0 & 0 & 0 & 1 & 0 & 0 \\ 0 & 0 & 0 & 0 & 1 & 0.02 \\ 0 & 0 & 0 & 0 & 0 & 1 \\ 0 & 0 & 0 & 0 & 0 & 0 \\ 0 & 0 & 0 & 0 & 0 & 0 \\ 0 & 0 & 0 & 0 & 0 & 0 \\ 0 & 0 & 0 & 0 & 0 & 0 \\ 0 & 0 & 0 & 0 & 0 & 0 \\ 0 & 0 & 0 & 0 & 0 & 0 \end{bmatrix}$$

$$\begin{bmatrix} 0 & 0 & 0 & 0 & 0 & 0 \\ 0 & 0 & 0.1962 & 0 & 0 & 0 \\ 0 & 0 & 0 & 0 & 0 & 0 \\ -0.1962 & 0 & 0 & 0 & 0 & 0 \\ 0 & 0 & 0 & 0 & 0 & 0 \\ 0 & 0 & 0 & 0 & 0 & 0 \\ 1 & 0.02 & 0 & 0 & 0 & 0 \\ 0 & 1 & 0 & 0 & 0 & 0 \\ 0 & 0 & 1 & 0.02 & 0 & 0 \\ 0 & 0 & 0 & 1 & 0 & 0 \\ 0 & 0 & 0 & 0 & 1 & 0.02 \\ 0 & 0 & 0 & 0 & 0 & 1 \end{bmatrix}, \quad (106)$$

$$B = \begin{bmatrix} 0 & 0 & 0 & 0 \\ 0 & 0 & 0 & 0 \\ 0 & 0 & 0 & 0 \\ 0 & 0 & 0 & 0 \\ 0 & 0 & 0 & 0 \\ 0.0005 & 0.0005 & 0.0005 & 0.0005 \\ 0 & 0 & 0 & 0 \\ -0.0137 & -0.0137 & 0.0137 & 0.0137 \\ 0 & 0 & 0 & 0 \\ -0.0137 & 0.0137 & 0.0137 & -0.0137 \\ 0 & 0 & 0 & 0 \\ 0.0007 & -0.0007 & 0.0007 & -0.0007 \end{bmatrix}, \quad (107)$$

and

$$C = \begin{bmatrix} 1 & 0 & 0 & 0 & 0 & 0 & 0 & 0 & 0 & 0 & 0 & 0 \\ 0 & 0 & 1 & 0 & 0 & 0 & 0 & 0 & 0 & 0 & 0 & 0 \\ 0 & 0 & 0 & 0 & 1 & 0 & 0 & 0 & 0 & 0 & 0 & 0 \\ 0 & 0 & 0 & 0 & 0 & 0 & 0 & 0 & 0 & 0 & 1 & 0 \end{bmatrix}. \quad (108)$$

The stabilizer gain computed by the *lqr* function of Matlab©is:

$$K = \begin{bmatrix} -0.4714 & 0.4714 & 0.4714 & -0.4714 \\ -0.8934 & 0.8934 & 0.8934 & -0.8934 \\ 0.4714 & 0.4714 & -0.4714 & -0.4714 \\ 0.8934 & 0.8934 & -0.8934 & -0.8934 \\ 0.4985 & 0.4985 & 0.4985 & 0.4985 \\ 3.3302 & 3.3302 & 3.3302 & 3.3302 \\ -5.9039 & -5.9039 & 5.9039 & 5.9039 \\ -2.1445 & -2.1445 & 2.1445 & 2.1445 \\ -5.9039 & 5.9039 & 5.9039 & -5.9039 \\ -2.1445 & 2.1445 & 2.1445 & -2.1445 \\ 0.4982 & -0.4982 & 0.4982 & -0.4982 \\ 2.7989 & -2.7989 & 2.7989 & -2.7989 \end{bmatrix}^T. \quad (109)$$

A. MATRICES FOR THE FIRST EXAMPLE

From (95) and (96), one gets;

$$S = \begin{bmatrix} 1 & 0.02 & 0 & 0 & 0 & 0 \\ 0 & 1 & 0.02 & 0 & 0 & 0 \\ 0 & 0 & 1 & 0.02 & 0 & 0 \\ 0 & 0 & 0 & 1 & 0.02 & 0 \\ 0 & 0 & 0 & 0 & 1 & 0.02 \\ 0 & 0 & 0 & 0 & 0 & 1 \\ 0 & 0 & 0 & 0 & 0 & 0 \\ 0 & 0 & 0 & 0 & 0 & 0 \\ 0 & 0 & 0 & 0 & 0 & 0 \\ 0 & 0 & 0 & 0 & 0 & 0 \\ 0 & 0 & 0 & 0 & 0 & 0 \\ 0 & 0 & 0 & 0 & 0 & 0 \end{bmatrix}$$

$$\begin{bmatrix} 0 & 0 & 0 & 0 & 0 & 0 \\ 0 & 0 & 0 & 0 & 0 & 0 \\ 0 & 0 & 0 & 0 & 0 & 0 \\ 0 & 0 & 0 & 0 & 0 & 0 \\ 0 & 0 & 0 & 0 & 0 & 0 \\ 0.02 & 0 & 0 & 0 & 0 & 0 \\ 1 & 0.02 & 0 & 0 & 0 & 0 \\ 0 & 1 & 0.02 & 0 & 0 & 0 \\ 0 & 0 & 1 & 0.02 & 0 & 0 \\ 0 & 0 & 0 & 1 & 0.02 & 0 \\ 0 & 0 & 0 & 0 & 1 & 0.02 \\ 0 & 0 & 0 & 0 & 0 & 1 \end{bmatrix}, \tag{110}$$

and

$$Q = \begin{bmatrix} 1 & 0 & 0 & 0 & 0 & 0 & 0 & 0 & 0 & 0 & 0 & 0 \\ 0 & 0 & 0 & 1 & 0 & 0 & 0 & 0 & 0 & 0 & 0 & 0 \\ 0 & 0 & 0 & 0 & 0 & 0 & 1 & 0 & 0 & 0 & 0 & 0 \\ 0 & 0 & 0 & 0 & 0 & 0 & 0 & 0 & 0 & 1 & 0 & 0 \end{bmatrix}. \tag{111}$$

Therefore, the solution of the Francis equations (20)-(21), with A, B, C, S, and Q as in (106). (107). (108). (110). and (111). respectively, and with $P_d = 0_{[12,12]}$ is:

$$\Pi = \begin{bmatrix} 1 & 0 & 0 & 0 & 0 & 0 \\ 0 & 1 & 0 & 0 & 0 & 0 \\ 0 & 0 & 0 & 1 & 0 & 0 \\ 0 & 0 & 0 & 0 & 1 & 0 \\ 0 & 0 & 0 & 0 & 0 & 0 \\ 0 & 0 & 0 & 0 & 0 & 0 \\ 0 & 0 & 0 & 0 & 0 & -0.1019 \\ 0 & 0 & 0 & 0 & 0 & 0 \\ 0 & 0 & 0.1019 & 0 & 0 & 0 \\ 0 & 0 & 0 & 0 & 0 & 0 \\ 0 & 0 & 0 & 0 & 0 & 0 \\ 0 & 0 & 0 & 0 & 0 & 0 \end{bmatrix}$$
$$\begin{bmatrix} 0 & 0 & 0 & 0 & 0 & 0 \\ 0 & 0 & 0 & 0 & 0 & 0 \\ 0 & 0 & 0 & 0 & 0 & 0 \\ 0 & 0 & 0 & 0 & 0 & 0 \\ 1 & 0 & 0 & 0 & 0 & 0 \\ 0 & 1 & 0 & 0 & 0 & 0 \\ 0 & 0 & 0 & 0 & 0 & 0 \\ 0 & 0 & 0 & 0 & 0 & 0 \\ 0 & 0 & 0 & 0 & 0 & 0 \\ 0 & 0 & 0 & 0 & 0 & 0 \\ 0 & 0 & 0 & 1 & 0 & 0 \\ 0 & 0 & 0 & 0 & 1 & 0 \end{bmatrix}, \tag{112}$$

and

$$\Gamma = \begin{bmatrix} 0 & 0 & 0 & 0 & 0 & 0 & 0 & 0 \\ 0 & 0 & 0 & 0 & 0 & 0 & 0 & 0 \\ 0 & 0 & 0 & 0 & 0 & 0 & 0 & 0 \\ 0 & 0 & 0 & 0 & 0 & 0 & 0 & 0 \\ 10.8419 & 0 & 0 & 7.5858 \\ 10.8419 & 0 & 0 & -7.5858 \\ 10.8419 & 0 & 0 & 7.5858 \\ 10.8419 & 0 & 0 & -7.5858 \end{bmatrix}. \tag{113}$$

B. MATRICES FOR THE SECOND EXAMPLE

For the sake of space, the overall matrices S, Q, Π, and Γ are not given in their common 2D representation, instead, the element-by-element representation is used, i.e.,

$$S = \in \mathbb{R}^{28\times 28} = \left[s_{i_s,j_s}\right], \tag{114}$$
$$Q = \in \mathbb{R}^{4\times 28} = \left[q_{i_q,j_q}\right], \tag{115}$$
$$\Pi = \in \mathbb{R}^{12\times 28} = \left[\pi_{i_\pi,j_\pi}\right], \tag{116}$$
$$\Gamma = \in \mathbb{R}^{4\times 28} = \left[\gamma_{i_\gamma,j_\gamma}\right], \tag{117}$$

with $i_s, j_s, j_q, j_\pi, j_\gamma = 1, \ldots, 28$, $i_\pi = 1, \ldots, 12$, $i_q, i_\gamma = 1, \ldots, 4$, $s_{1,1} = s_{2,2} = s_{3,3} = s_{4,4} = s_{5,5} = s_{6,6} = s_{7,7} = s_{8,8} = s_{9,9} = s_{10,10} = s_{11,11} = s_{12,12} = s_{13,13} = s_{14,14} = s_{15,15} = s_{16,16} = s_{17,17} = s_{18,18} = s_{19,19} = s_{20,20} = s_{21,21} = s_{22,22} = s_{23,23} = s_{24,24} = s_{25,25} = s_{26,26} = s_{27,27} = s_{28,28} = q_{1,1} = q_{2,8} = q_{3,15} = q_{4,22} = \pi_{1,1} = \pi_{2,2} = \pi_{3,8} = \pi_{4,9} = \pi_{5,15} = \pi_{6,16} = \pi_{11,22} = \pi_{12,23} = 1$, $s_{1,2} = s_{2,3} = s_{3,4} = s_{4,5} = s_{5,6} = s_{6,7} = s_{8,9} = s_{9,10} = s_{10,11} = s_{11,12} = s_{12,13} = s_{13,14} = s_{15,16} = s_{16,17} = s_{17,18} = s_{18,19} = s_{19,20} = s_{20,21} = s_{22,23} = s_{23,24} = s_{24,25} = s_{25,26} = s_{26,27} = s_{27,28} = 0.02$, $\pi_{9,3} = \pi_{10,4} = 0.1019$, $\pi_{7,10} = \pi_{8,11} = -0.1019$, $\gamma_{1,5} = \gamma_{4,5} = \gamma_{3,12} = \gamma_{4,12} = -0.0373$, $\gamma_{2,5} = \gamma_{3,5} = \gamma_{1,12} = \gamma_{2,12} = 0.0373$, $\gamma_{1,17} = \gamma_{2,17} = \gamma_{3,17} = \gamma_{4,17} = 10.8419$, $\gamma_{1,24} = \gamma_{3,24} = 7.5858$, $\gamma_{2,24} = \gamma_{4,24} = -7.5858$. The rest of the elements of the matrices S, Q, Π, and Γ are equal to zero.

REFERENCES

[1] C. K. Chui and G. Chen, *Kalman Filtering With Real-Time Applications*. Berlin, Germany: Springer-Verlag, 1987.

[2] T. Kailath, *Linear Systems*. Englewood Cliffs, NJ, USA Prentice-Hall, 1980.

[3] C.-T. Chen, *Linear System Theory and Design*. New York, NY, USA: Oxford Univ. Press, 1998.

[4] A. Isidori and C. I. Byrnes, "Output regulation of nonlinear systems," *IEEE Trans. Autom. Control*, vol. 35, no. 2, pp. 131–140, Feb. 1990, doi: 10.1109/9.45168.

[5] A. Isidori, *Nonlinear Control Systems*, 3rd ed. London, U.K.: Springer-Verlag, 1995.

[6] B. Francis, "The linear multivariable regulator problem," in *Proc. IEEE Conf. Decis. Control, 15th Symp. Adapt. Processes*, Clearwater, FL, USA, Dec. 1976, pp. 873–878, doi: 10.1109/CDC.1976.267849.

[7] C. J. Boss, V. Srivastava, and H. K. Khalil, "Robust tracking of an unknown trajectory with a multi-rotor UAV: A high-gain observer approach," in *Proc. Amer. Control Conf. (ACC)*, Denver, CO, USA, Jul. 2020, pp. 1429–1434, doi: 10.23919/ACC45564.2020.9147979.

[8] T. Hernández-Cortés, M. Amador-Macias, R. Tapia-Herrera, and J. A. Meda-Campaña, "On the output regulation for an underactuated inverse pendulum when the exosystem is a high-gain observer," *IEEE Access*, vol. 11, pp. 10792–10800, 2023, doi: 10.1109/ACCESS.2023.3240656.

[9] J. A. Meda-Campaña, R. I. Ancona-Bravo, J. O. Escobedo-Alva, T. Hernández-Cortés, and R. Tapia-Herrera, "The output regulation problem for unmodeled reference/disturbance signals using high-gain observers," *Int. J. Control Autom. Syst.*, vol. 21, pp. 1049–1061, Mar. 2023, doi: 10.1007/s12555-021-0766-9.

[10] H. K. Khalil, *High-gain Observers in Nonlinear Feedback Control*. Philadelphia, PA, USA: Society for Industrial and Applied Mathematics, 2017.

[11] J. A. Meda-Campaña, "On the estimation and control of nonlinear systems with parametric uncertainties and noisy outputs," *IEEE Access*, vol. 6, pp. 31968–31973, 2018, doi: 10.1109/ACCESS.2018.2846483.

[12] C. Zheng, M. Yu, J. Shan, A. Wang, and H. Chen, "Fast sparse non-negative least squares via ADMM for high resolution DOA estimation," *IEEE Sensors J.*, vol. 23, no. 4, pp. 3901–3910, Feb. 2023, doi: 10.1109/JSEN.2022.3233820.
[13] J. A. Meda-Campaña, J. O. Escobedo-Alva, J. D. J. Rubio, C. Aguilar-Ibañez, J. H. Perez-Cruz, G. Obregon-Pulido, R. Tapia-Herrera, E. Orozco, D. A. Cordova, and M. A. Islas, "On the rejection of random perturbations and the tracking of random references in a quadrotor," *Complexity*, vol. 2022, pp. 1–16, Jan. 2022, doi: 10.1155/2022/3981340.
[14] S. Bazm, P. Lima, and S. Nemati, "Analysis of the Euler and trapezoidal discretization methods for the numerical solution of nonlinear functional Volterra integral equations of Urysohn type," *J. Comput. Appl. Math.*, vol. 398, Dec. 2021, Art. no. 113628, doi: 10.1016/j.cam.2021.113628.
[15] L. A. Paramo, E. C. Garcia, J. A. Meda, J. D. J. Rubio, J. O. Escobedo, R. Tapia, J. O. Hernandez, G. Lopez, J. F. Novoa, and A. Aguilar, "Quadrotor stabilization by fuzzy Kalman filter," *J. Intell. Fuzzy Syst.*, vol. 38, no. 4, pp. 4485–4494, Apr. 2020, doi: 10.3233/JIFS-191251.
[16] R. Srivastava, R. Lima, R. Sah, and K. Das, "In-orbit control of floating space robots using a model dependant learning based methodology," in *Proc. IEEE Aerosp. Conf.*, Big Sky, MT, USA, Mar. 2023, pp. 1–10, doi: 10.1109/AERO55745.2023.10115732.

JESÚS ALBERTO MEDA-CAMPAÑA (Member, IEEE) received the B.Sc. degree (Hons.) in computer engineering from Instituto Tecnológico y de Estudios Superiores de Monterrey (ITESM), Culiacán, Sinaloa, Mexico, in 1993, and the M.Sc. and Ph.D. degrees in electrical engineering from Centro de Investigación y de Estudios Avanzados del Instituto Politécnico Nacional (CINVESTAV-IPN), Guadalajara, Jalisco, Mexico, in 2002 and 2006, respectively. He is a full-time Professor with the Department of Mechanical Engineering, Sección de Estudios de Posgrado e Investigación, Escuela Superior de Ingenieria Mecánica y Eléctrica, Instituto Politécnico Nacional, Mexico City, Mexico. He has authored/coauthored more than 70 papers in journals and conferences. He has supervised one postdoctoral researcher, 16 Ph.D., and 22 M.Sc. theses. He is currently supervising six Ph.D. and three M.Sc. students. His main research interests include linear and nonlinear control design, fuzzy regulation theory, optimal control, and the application of control techniques to electromechanical systems and robotics.

RAÚL EDUARDO TORRES-CRUZ received the B.Sc. degree in mechanical engineering from Escuela Superior de Ingeniería Mecánica y Eléctrica Campus Culhuacán, Instituto Politécnico Nacional, Mexico City, in 2022, where he is currently pursuing the degree in mechanical engineering with Sección de Estudios de Posgrado e Investigación, Escuela Superior de Ingeniera Mecánica y Eléctrica Campus Zacatenco. His research interests include control of nonlinear systems, output regulation theory, robotics, fuzzy systems, and real-time applications.

ALEXIS JESUS ROJAS-RUIZ received the B.Sc. degree in mechanical and electrical engineering from Benemérita Universidad Autónoma de Puebla (BUAP), Puebla, Mexico, in 2019. He is currently pursuing the master's degree in mechanical engineering with Sección de Estudios de Posgrado e Investigación (SEPI), Escuela Superior de Ingeniería Mecánica y Eléctrica (ESIME), Instituto Politécnico Nacional (IPN). His research interests include linear and nonlinear control design, regulation theory, and robotics and mechanical design.

RICARDO TAPIA-HERRERA (Member, IEEE) received the B.Sc. degree in industrial robotics engineering from Instituto Politécnico Nacional (IPN), Mexico, in 2005, and the M.Sc. and Ph.D. degrees in mechanical engineering from IPN-SEPI ESIME Zacatenco, in 2009 and 2013, respectively. Currently, he is a Visiting Researcher with IPN, where he is participating in the program of CONACYT "Investigadores por México" with the research project, design and control of robots and automated systems for vaccine development. His areas of interests are fuzzy control, mechanical design, robotics, analysis, synthesis, and dynamics of mechanisms. His main research interests include the design of nonlinear controllers, neuro-fuzzy systems in output regulation problems, and the application of control techniques to mechatronic systems.

TONATIUH HERNÁNDEZ-CORTÉS received the B.Sc. degree in robotics from Escuela Superior de Ingeniería Mecánica y Eléctrica Campus Azcapotzalco, Instituto Politécnico Nacional, Mexico City, Mexico, in 2005, and the M.Sc. and Ph.D. degrees in mechanical engineering from Sección de Estudios de Posgrado e Investigación, Escuela Superior de Ingeniería Mecánica y Eléctrica Campus Zacatenco, Instituto Politécnico Nacional, in 2012 and 2016, respectively. He is currently a Full Professor with the Department of Mechatronic Engineering, Universidad Politécnica de Pachuca, Zempoala, Mexico. His research interests include control of nonlinear systems, output regulation theory, robotics, fuzzy systems, and real-time applications.

LUIS ALBERTO PÁRAMO-CARRANZA received the B.Sc. degree in mechatronics from Unidad Profesional Interdiscilinaria en Ingeniería y Tecnologías Avanzadas (UPIITA), Instituto Politécnico Nacional (IPN), Mexico City, Mexico, in 2007, and the M.Sc. and Ph.D. degrees in mechanical engineering from Sección de Estudios de Posgrado e Investigación, Escuela Superior de Ingeniería Mecánica y Eléctrica Zacatenco, IPN, Campus Zacatenco, Mexico City, in 2014 and 2019, respectively. He was a Postdoctoral Researcher with Universidad Iberoamericana, Mexico City. He is currently a Professor with the Department of Control, Communications and Electronics Engineering, Escuela Superior de Ingeniería Mecánica y Eléctrica, IPN, Campus Zacatenco. His research interests include control of nonlinear systems, neural networks, fuzzy systems, Kalman filter, robotics, and mechatronics.